

# Surface temperature effects in dynamic trapping mediated adsorption of light molecules on metal surfaces: H<sub>2</sub> on Pd(111) and Pd(110)

H. F. Busnengo,<sup>1,\*</sup> M. A. Di Césare,<sup>2</sup> W. Dong,<sup>3</sup> and A. Salin<sup>4</sup>

<sup>1</sup>*Instituto de Física Rosario (CONICET-UNR) and Facultad de Ciencias Exactas, Ingeniería y Agrimensura, Universidad Nacional de Rosario, Avenida Pellegrini 250, 2000 Rosario, Argentina*

<sup>2</sup>*Instituto de Física Rosario (CONICET-UNR), Avenida Pellegrini 250, 2000 Rosario, Argentina*

<sup>3</sup>*Ecole Normale Supérieure de Lyon, 46 Allée d'Italie, F-69364 Lyon Cedex 07, France*

<sup>4</sup>*Laboratoire de Physico-Chimie Moléculaire, UMR 5803 CNRS-Université Bordeaux I, 351 Cours de la Libération, 33405 Talence Cedex, France*

(Received 11 May 2005; published 8 September 2005)

We perform classical trajectory calculations on nonactivated H<sub>2</sub> dissociative adsorption on Pd surfaces, using the surface oscillator model to account for phonons. We show that the role of surface temperature is closely related to the dynamic trapping process that enhances energy exchange with the surface by increasing considerably the interaction time before dissociation or reflection. Correlatively, the trapping process itself is enhanced by energy loss to the surface while it is quenched by energy gain. We show that, for a hot surface, isotopic effects in temperature dependencies are driven by the enhanced interaction time when the mass increases for a given energy and not by the ratio of molecule mass to that of surface atoms. Finally, we find that introduction of energy dissipation toward the bulk through generalized Langevin oscillators gives rise to molecular adsorption.

DOI: [10.1103/PhysRevB.72.125411](https://doi.org/10.1103/PhysRevB.72.125411)

PACS number(s): 68.43.-h, 79.20.Rf, 34.50.Dy, 82.65.+r

## I. INTRODUCTION

Our comprehension of dynamical processes in molecule/surface interactions has progressed significantly thanks to the development of density functional theory (DFT) that allows a routine determination of the potential energy surfaces (PES) for a molecule in front of a rigid surface. In principle, it is even possible, through *ab initio* molecular dynamics, to determine, on the fly, the evolution of the system electronic state associated with the dynamical evolution of both the molecule and surface atoms. Still, the latter method is computationally intensive, which explains why most studies on dissociative adsorption of molecules were carried out for a frozen surface, i.e., neglecting molecule/phonon energy exchange (see Refs. 1 and 2 and references therein). For the case of H<sub>2</sub>, this procedure has usually been justified by invoking the mass mismatch between the molecule and surface atoms. Experimental evidence<sup>3,4</sup> on the weak dependence of sticking probabilities on surface temperature,  $T_s$ , was also used as a confirmation of the weak coupling between molecular and surface degrees of freedom (DOF). However, recent molecular beam experiments have shown that low-energy H<sub>2</sub> molecules may exchange large amounts of energy with surface phonons, even for systems for which the sticking probability presents a weak  $T_s$  dependence.<sup>5,6</sup> These observations have renewed interest in the role of energy exchange with phonons for light molecules.

The first theoretical attempts to understand  $T_s$  effects in sticking of light molecules on metal surfaces were stimulated by measurements of energy and angular distributions of D<sub>2</sub> molecules desorbing from Cu(111).<sup>7,8</sup> The initial sticking probability as a function of incidence energy,  $S(E_i)$ , was derived from the latter measurements by the application of a detailed balance and the use of an analytic form for  $S(E_i)$ ,

assumed *a priori* to be generic for activated dissociation. The S-like curve thus obtained for  $S(E_i)$  broadens with increasing  $T_s$ . At energies close to threshold, a clear enhancement of the sticking probability is also observed when heating the surface.<sup>7,8</sup> The simplest method accounting for molecule-surface energy exchange is the surface oscillator (SO) model.<sup>9,10</sup> In the latter, a single harmonic oscillator of frequency  $\omega$  is used to represent surface vibrations and the motion of this oscillator couples to molecular motion via a rigid shift of the PES along the oscillator coordinate.<sup>9,10</sup> Despite its simplicity, the SO model successfully accounts<sup>11–13</sup> for the  $T_s$  dependence of the experimental sticking probability.<sup>7,8</sup>

As far as theory is concerned, much less attention has been paid to  $T_s$  effects in H<sub>2</sub> sticking on more reactive surfaces for which dissociation is nonactivated.<sup>44</sup> In the latter case, at low energies, the sticking probability is large and barely depends on  $T_s$ . It is to note, however, that a slight decrease of adsorption with  $T_s$  (Refs. 14–16) has been observed in some cases, in contrast with the increase observed for H<sub>2</sub>/Cu. The reaction mechanisms responsible for the nonactivated adsorption of H<sub>2</sub> on metals at low energies has been a matter of debate over the last years (see, e.g., Refs. 15–32). There exists experimental and theoretical evidence of an *indirect* mechanism for the dissociation of H<sub>2</sub> on several metal surfaces.<sup>16,21,27–32</sup> At low energies (below  $\sim 0.1$ – $0.15$  eV) two mechanisms contribute to dissociation: *direct* and *indirect (dynamic trapping)*. Whereas some molecules dissociate directly when approaching the surface (direct mechanism), others spend a long time close to the surface, undergo many rebounds, and explore a large surface area before dissociation (dynamic trapping). With increasing impact energy, the role of dynamic trapping decreases and, eventually, dissociation only takes place through a direct mechanism. Dynamic trapping can be considered as the *mo-*

bile precursor for dissociation invoked by many authors in the past, but in contrast with the usual picture of a *precursor state*, dynamic trapping is due to energy transfer from translation perpendicular to the surface to other molecular DOFs and does not require energy loss to the surface. Dynamic trapping allows us to explain the increase of the sticking probability when  $E_i$  decreases at low energies.<sup>29–31</sup> For the present study, the most important feature of dynamic trapping is the associated long  $H_2$ -surface interaction time, before reflection or dissociation, which allows an efficient energy exchange with phonons.<sup>33</sup>

Experimentally, it is not trivial to sort out the contributions of direct and indirect mechanisms and this may be dependent on the reactivity of the system.<sup>16,31</sup> In particular, dynamic trapping may dominate at low energies for adsorption and reflection in systems characterized by a small number of nonactivated paths to dissociation. It might be possible to observe its fingerprint, for instance, in the angular distribution of reflected molecules.<sup>16,21,27,31,34</sup>

Whereas the effect of energy exchange with phonons on direct adsorption might be expected to be the same as for activated dissociation, its effect on dynamic trapping is less obvious for light molecules. Mass mismatch and long interaction times are competing factors and the overall effect might be strongly influenced by the PES shape. Moreover, the fact that, in general, adsorption takes place at low energies through both direct and indirect mechanisms,<sup>29,31</sup> makes it more difficult to predict the net effect of  $T_s$ . It is our objective in this present paper to shed some light on these issues. To the best of our knowledge, there has been no detailed theoretical study, until now, of  $T_s$  effects in  $H_2$  nonactivated adsorption, and, even more generally (i.e., for activated adsorption as well) using an *ab initio* PES that takes into account all molecular DOF.

The present work is based on our previous work in which the 6D PES for  $H_2/Pd(111)$  and  $H_2/Pd(110)$  have been determined with DFT and the dissociative adsorption process has been studied in depth for the rigid surface (RS) model.<sup>28,29,31,35</sup> Surface temperature effects are studied with the SO model. One limitation of the latter is in the absence of coupling with the bulk, which implies energy conservation for the ensemble  $SO+H_2$ . One most efficient way to account for energy exchange with the bulk is to consider the generalized Langevin oscillators (GLO)<sup>9,36</sup> model. The latter model has been used in a large body of contributions to represent the interaction of the surface layer(s) and adsorbates with the “thermal bath” provided by the bulk.

Finally, we would like to stress that our ambition is less in simulating or making quantitative predictions for conditions relevant to measurements than in understanding the mechanisms through which temperature effects can be effective in nonactivated dissociation. In this respect, further DFT calculations with the projector augmented wave (PAW) method give rise to a more reactive PES for  $H_2/Pd(110)$  compared to that obtained previously with ultrasoft pseudopotentials (US),<sup>31</sup> the one used in the present calculations. Even though the reactivity might be underestimated, this is an advantage for our purpose, which is to compare  $T_s$  effects in nonactivated systems with different reactivities.

## II. METHODS

The present classical trajectory calculations for  $H_2/Pd(111)$  and  $H_2/Pd(110)$  are based on the six-dimensional PES’ previously used in Ref. 31 for the rigid surface (RS) model. We perform C-ZPE calculations as defined in Ref. 29. The initial internuclear distance in the molecule is assumed to be fixed at its equilibrium value, as in so-called “classical calculations.” However, the effect of the vibrational zero-point energy (ZPE) variation in the entrance channel is accounted for as in Eq. (3) of Ref. 31. The validity of this method has been previously shown through the comparison with quantum results using the same PES for  $H_2/Pd(111)$  within the RS model.<sup>30,32</sup>

A particular configuration of the molecule in front of the rigid surface is defined by the Cartesian coordinates of its center of charge  $X$ ,  $Y$ ,  $Z$ —with the  $Z$  axis normal to the surface, pointing toward vacuum, and the  $X$  axis along the line connecting two nearest surface atoms—the internuclear distance,  $r$ , the polar,  $\theta$ , and azimuthal,  $\varphi$ , angles of the internuclear axis. Alternatively, one may use the Cartesian coordinates  $\mathbf{R}_A(X_A, Y_A, Z_A)$  and  $\mathbf{R}_B(X_B, Y_B, Z_B)$  of the nuclei  $A$  and  $B$ .

The surface oscillator (SO) model represents the surface motion in terms of a single 3D harmonic oscillator of mass  $m_s$  with coordinates  $\mathbf{R}_s(X_s, Y_s, Z_s)$  and associated  $3 \times 3$  frequency matrix  $\hat{\Omega}_s$ . The  $H_2$  phonon coupling is described by a space rigid shift  $\mathbf{R}_s$  of the 6D potential energy surface,  $V_{6D}(\mathbf{R}_A, \mathbf{R}_B)$ , for the molecule in front of the rigid surface, i.e.,

$$V_{SO}(\mathbf{R}_A, \mathbf{R}_B; \mathbf{R}_s) = V_{6D}(\mathbf{R}_A - \mathbf{R}_s, \mathbf{R}_B - \mathbf{R}_s). \quad (1)$$

The generalized Langevin oscillator (GLO) model adds dissipation and thermal fluctuations with the help of a ghost 3D oscillator with coordinate  $\mathbf{U}(U_x, U_y, U_z)$  and associated frequency matrix  $\hat{\omega}_g$ . The ghost oscillator and surface oscillator are coupled by a coupling matrix  $\hat{\Lambda}_{gs}$ . In addition, the ghost oscillator is subject to a friction force with damping matrix  $\hat{\gamma}_g$  and to a random force  $\mathbf{W}(\Delta t)$ . The latter is a Gaussian white noise source with variance  $(2k_B T_s \gamma_g / m_s \Delta t)^{1/2}$ . Here,  $\Delta t$  is the time integration step and  $k_B$  is the Boltzmann constant. With these definitions, the equations of motion for the 12 coordinates characterizing the system read as

$$\frac{d^2 \mathbf{R}_{A,B}}{dt^2} = - \frac{1}{m_{A,B}} \nabla_{\mathbf{R}_{A,B}} V_{6D}(\mathbf{R}_A - \mathbf{R}_s, \mathbf{R}_B - \mathbf{R}_s), \quad (2)$$

$$\frac{d^2 \mathbf{R}_s}{dt^2} = - \frac{1}{m_s} \nabla_{\mathbf{R}_s} V_{6D}(\mathbf{R}_A - \mathbf{R}_s, \mathbf{R}_B - \mathbf{R}_s) - \hat{\Omega}_s^2 \mathbf{R}_s + \hat{\Lambda}_{gs} \mathbf{U}, \quad (3)$$

$$\frac{d^2 \mathbf{U}}{dt^2} = - \hat{\omega}_g^2 \mathbf{U} + \hat{\Lambda}_{gs} \mathbf{R}_s - \hat{\gamma}_g \frac{d\mathbf{U}}{dt} + \mathbf{W}(\Delta t). \quad (4)$$

Equations (2)–(4) are the same as those of Refs. 36 and 9, except for a small change in notations. In contrast with Ref. 9, the 3D ghost oscillator moves in three dimensions. An alternative channel for energy transfer to the surface, not

accounted for by the GLO model, is electron-hole pair creation whose role in the  $H_2$ -metal surface dynamics is still not well established.<sup>1,2</sup>

The SO model is obtained from the GLO model by eliminating any reference to  $\mathbf{U}$  in Eqs. (3) and (4). The system is, then, conservative and characterized by nine coordinates (the six molecular DOFs, and three for the surface oscillator). The RS model is obtained from the SO model by setting  $\mathbf{R}_s=0$ . For the time integration in the RS and SO models we have used the predictor-corrector method of Burlisch and Stoer<sup>37</sup> whereas for the GLO model we have used the third-order procedure of Beeman<sup>38</sup> as in the work of Tully *et al.*<sup>39</sup> From now on, we use the subscripts RS, SO, and GLO to label the probabilities obtained with the corresponding model.

### III. RESULTS AND DISCUSSIONS

We discuss first our results in the SO model that allow us to understand more easily the main trends in the role of molecule/phonon energy exchange. The additional specific role of dissipation to the bulk will be discussed in the following section on the GLO model.

#### A. Parameters

We have first to fix the values of the parameters for the SO and GLO models. First of all, we have assumed that all matrices in Eqs. (3) and (4) are diagonal. For a more direct comparison between Pd(111) and Pd(110), we have employed the same surface oscillator frequencies for both surfaces:<sup>33</sup>  $\Omega_{p,X}^2=\Omega_{p,Y}^2=6 \times 10^{-4}$  and  $\Omega_{p,Z}^2=4 \times 10^{-4}$  (in a.u.). The same values are used for the ghost oscillators. In fact, our results are not sensitive to  $\Omega_p$ . For  $\Omega_p \rightarrow \infty$  the RS model is regained. This is also the case for  $\Omega \rightarrow 0$ , except that the  $H_2$  mass is then replaced by the  $H_2$ /oscillator reduced mass.<sup>45</sup> The SO/RS difference only appears for  $\Omega_p$  in the range ( $5 \times 10^{-5}, 5 \times 10^{-2}$ ). In this range, all qualitative behaviors described below are the same; only the absolute magnitudes change with a maximum effect observed around the above values. For example, when  $T_s=10$  K, the dissociation probability for a 10 meV  $H_2$  incident on the (111) surface is 0.967 for  $\Omega_p=6 \times 10^{-5}$ , 0.944 for  $\Omega_p=6 \times 10^{-4}$ , and 0.974 for  $\Omega_p=6 \times 10^{-3}$ . The corresponding figures are 0.93, 0.9, and 0.92 for  $T_s=800$  K. The GLO model relies on the damping factor  $\gamma$ , which we assume isotropic. Results given below are for  $\gamma \sim \pi\omega_D/6 \sim 4.5 \times 10^{-4}$  a.u., where  $\omega_D$  is the Pd Debye frequency, as proposed by Adelman and Doll.<sup>40</sup> We have run calculations at low energies (when the SO/RS difference is maximum) for  $\gamma=4.5 \times 10^{-n}$ , with  $n$  varying from 3 to 6, and no significant difference was found. In addition, the discussion below allows us to sort out the role of dissipation and, thus, predict the outcome of increasing or decreasing even more the value of  $\gamma$ . In general, for each value of  $E_i$  and  $T_s$  we have computed 10 000 trajectories (50 000 for Fig. 6) that allow us to obtain statistical errors lower than approximately 1%, which is enough for our purposes.

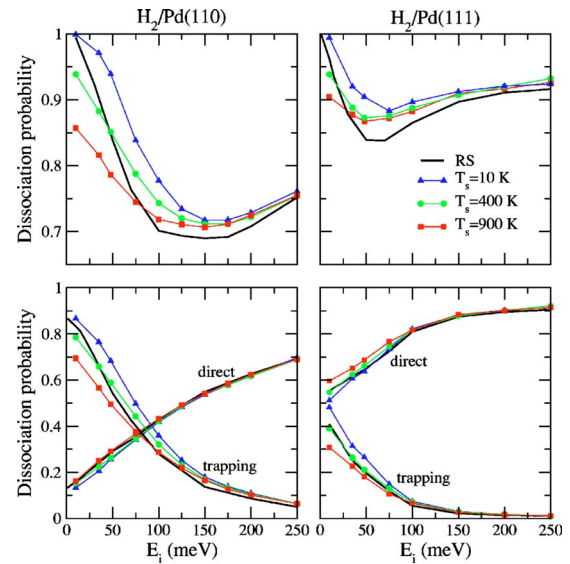


FIG. 1. (Color online) Dissociative adsorption probability of  $H_2$  on the Pd(110) (left) and Pd(111) (right) surfaces as a function of impact energy, calculated in the surface oscillator (SO) model for various surface temperatures. Results for the rigid surface (RS) are given for the sake of comparison. Upper panels give the total probability and lower panels their decomposition in terms of direct and trapping contributions.

#### B. SO model

##### 1. Energy exchange and trapping

Figure 1 shows the dissociative adsorption probability,  $P_{diss}$ , of  $H_2(J=0)$  on Pd(111) and Pd(110) as a function of the impact energy obtained for various surface temperatures. They do not agree with those of the RS model, even at very low surface temperatures, a clear measure of the role of energy transfer between the molecule and the surface. The  $T_s$  effect is, in general, weak, being more important for  $H_2/Pd(110)$  than for  $H_2/Pd(111)$ . It is larger at low energies, where  $P_{diss}$  decreases when  $T_s$  increases. For  $E_i > 150$  meV, the adsorption probability is nearly independent of  $T_s$  and close to that of the RS model.

To understand the origin of the surface temperature dependence at low energies, it is useful to study separately the contribution of direct and indirect (dynamic trapping) mechanisms. A simple way to discriminate them is through the number of rebounds on the surface,  $N_{reb}$ . We consider that a trajectory has been trapped when  $N_{reb} > 5$ . The lower panels in Fig. 1 give the decomposition of the dissociation probability in terms of the trapping contribution (molecules that dissociate after at least five rebounds) and the complementary “direct” one. They show that the temperature effect is far more important for the trapping contribution and that an increase in temperature decreases the dissociation probability through trapping.

Let us call  $P^{trap}$  the fraction of trajectories for which  $N_{reb} > 5$ , whether they lead to dissociation or not. The temperature dependence of the trapping probability for the (110) surface is given in Fig. 2. Similar results are obtained for  $H_2/Pd(111)$ . It can be seen that  $P^{trap}$  always decreases when



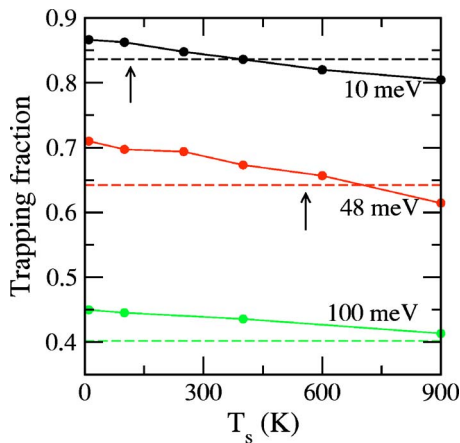


FIG. 2. (Color online) Fraction of trajectories in H<sub>2</sub> impact on Pd(110) involving trapping before dissociation or reflection as a function of surface temperature and for various impact energies. Arrows represent the value of  $T_s$  such that  $k_B T_s = E_i$ . Dashed lines correspond to the value for a rigid surface.

$T_s$  increases, though its magnitude never differs much from the value for the RS. We recall that dynamic trapping, for a rigid surface, is a direct consequence of the attractive character of the PES far from the surface. The transfer of energy from perpendicular motion to other molecular DOFs, due to the surface anisotropy when the molecule approaches the surface, may prevent the molecule from climbing back from the PES slope toward the vacuum. This effect is at a maximum for very low energies since the whole transferred energy must then be given back to normal motion to make reflection possible (see the discussion in Ref. 31). This particular form of trapping does not involve energy exchange with the surface and has been accordingly named “elastic” trapping.<sup>41</sup> In addition, one may easily understand how inelastic processes may influence the trapping mechanism. Energy loss by the molecule will enhance trapping since it will make it even more difficult for the molecule to climb back the potential toward the vacuum. Such an enhancement might be referred to as “inelastic” trapping. On the converse, energy gain will help reflection and therefore damp the trapping mechanism. The fact that the trapping probability does not differ much from the rigid surface value shows that the trapping process is still essentially due to the 6D dynamics (i.e., to energy exchange between molecular DOFs as in the RS model). Thus, the *dynamic* or *elastic* trapping is the basic process at work. With these ideas in mind, it is easy to understand the origin of the temperature dependence.

The vertical arrows in Fig. 2 indicate the values of  $T_s$  for which  $k_B T_s = E_i$ : 116 K for  $E_i = 10$  meV and 557 K for  $E_i = 48$  meV (it would be 1160 K for  $E_i = 100$  meV). When  $E_i > k_B T_s$ , the energy involved in normal motion makes the molecule initially *hot* compared with the surface. One may expect that, on average, the molecule will transfer energy to the surface. As lowering the kinetic energy of the molecule enhances trapping,  $P_{SO}^{trap} > P_{RS}^{trap}$  when  $E_i > k_B T_s$ . On the other hand, when  $E_i < k_B T_s$  molecules are initially *cold* (compared with the surface) and will be more likely to receive energy from the surface. In this case,  $P_{SO}^{trap} < P_{RS}^{trap}$ , in agreement with the expected decrease of trapping when the kinetic energy of

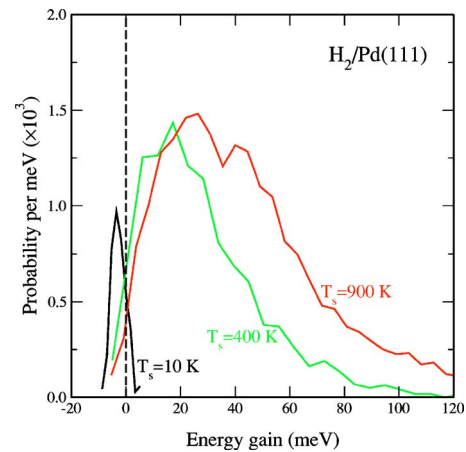


FIG. 3. (Color online) Reflection probability per meV of energy gain for H<sub>2</sub> molecules reflected from the Pd(111) surface. Impact energy is 10 meV.

the molecule increases. This can be proved quantitatively by looking at the distribution of energy gains by reflected molecules as shown in Fig. 3 for 10 meV impact on the (111) surface. For 10 K, the energy transfer goes essentially from the molecule toward the surface and the converse is true for 400 and 900 K.

After gaining insight into the relation between energy exchange and trapping, we turn now to the relative yield of dissociation and reflection. This is shown in Fig. 4 for Pd(110). The most striking result is that the temperature ef-

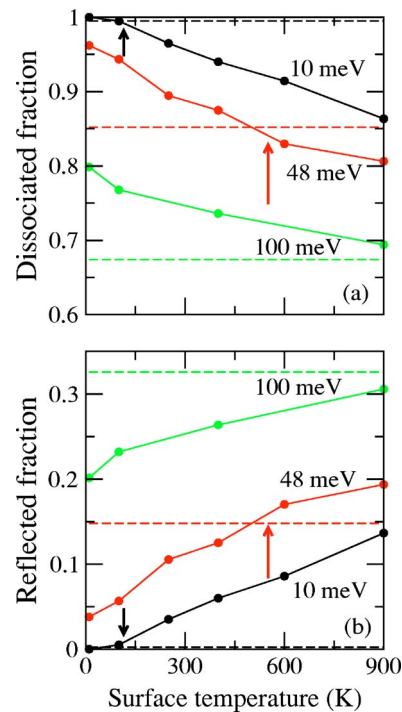


FIG. 4. (Color online) Fraction of trapping trajectories in H<sub>2</sub> impact on Pd(110) leading to dissociation (a) or reflection (b) as a function of temperature and for various impact energies. Arrows represent the value of  $T_s$  such that  $k_B T_s = E_i$ . Dashed lines correspond to the value for a rigid surface.

fect on dissociation through trapping [Fig. 4(a)] is enhanced with respect to the effect on global trapping of Fig. 2, which goes along with a correlative increase of reflection associated with trapping [Fig. 4(b)]. In fact, this trend can be easily understood. For  $E_i > k_B T_s$ , energy loss to the surface is often large enough to quench reflection while for  $E_i < k_B T_s$  energy gain will help a larger fraction of the trapped molecules to go back into the vacuum, explaining the regular increase of the reflected fraction with temperature. The latter effect provokes a dramatic increase with temperature, for low impact energies, in the fraction of reflected molecules that have suffered trapping, as seen in Fig. 5. For the case of the (111) surface, no variation with temperature is observed for reflected molecules because of the higher reactivity of the latter surface that entails that nearly all trapped trajectories lead to dissociation.

It is possible to confirm this role of dynamic trapping in molecule/surface energy exchange by looking at the energy exchange as a function of the rebound number. The latter quantity can only be defined unambiguously for reflected molecules because in their final state they do not interact with the surface. For each reflected molecule we note the total rebound number and the associated energy change. The latter is plotted as a function of the former in Fig. 6 for the (111) surface. We observe that it first increases and then reaches a “saturation” value, indicating that a quasiequilibrium has been reached for a large enough rebound number: in further recollisions with the surface, the energy gains are, on average, compensated by losses. When the incident molecule is hot with respect to the surface, energy exchange does go from the molecule toward the surface, and *vice versa*. Also, the hotter the surface the larger the equilibrium value of the energy gain.

## 2. Connection with experiment

In the case of initial sticking of  $H_2$  on Pd surfaces, measurements can be carried out for a temperature window of 400–900 K. We consider first the case of Pd(111). For a nonrotating molecule, we predict a variation in the latter  $T_s$  interval of only  $\sim 5\%$  for  $E_i < 25$  meV and an almost negligible one for higher energies (see Fig. 1). Moreover, we found an even smaller  $T_s$  effect for initially rotating molecules because of the decreasing role of trapping. As  $H_2$  beams usually involve a majority of rotationally excited molecules, we would not expect any effect of  $T_s$  on the measured sticking probability. We found stronger  $T_s$  effects for the (110) surface because of the more important role of dynamic trapping in the latter case:<sup>31</sup> the decrease in  $P_{diss}$  is approximately 10% as  $T_s$  goes from 400 to 900 K and for the lowest energies. It is negligible for energies above 150 meV. In addition, dynamic trapping is less sensitive to the initial value of  $J$ . We would therefore expect a measurable reduction of the sticking probability with increasing  $T_s$ , in line with the experimental result for  $H_2/W(100)-c(2 \times 2)Cu$ <sup>16,21</sup> in which the dissociative adsorption takes place almost exclusively via dynamic trapping at low energies. A decrease of the sticking probability with increasing temperature has also been observed for  $H_2$  dissociation on Ni(110)<sup>14</sup> and W(100)<sup>15</sup> at low

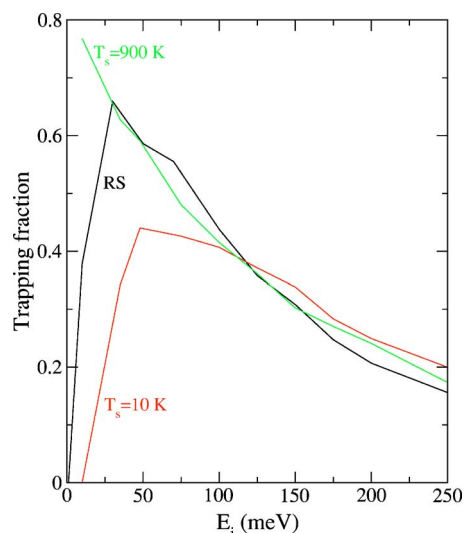


FIG. 5. (Color online) Fraction of reflected molecules that have been trapped as a function of impact energy.

impact energies, where the dissociation probability for these systems is decreasing with energy. If the latter behavior is considered as a clue that trapping is effective, the interpretation of the temperature dependence is consistent with the above discussion.

## 3. Mass effect

It is usually assumed that the mass ratio between the projectile and surface atoms is the key factor governing energy exchange with surface phonons. In Ref. 33, it has been already pointed out that the interaction time plays an important role. We show, in the present section, how the relative importance of these two factors can be estimated.

In a first step, we have performed calculations for deuterium and tritium molecules for both a rigid surface and a surface with a temperature of 900 K. Results are plotted in Fig. 7 for Pd(110). For the rigid surface, the difference between calculations for  $H_2$ ,  $D_2$ , and  $T_2$  is negligible at low energies. It is at maximum for impact energies around 150 meV and decreases slowly at larger energies. For the hot surface, no difference is observed above 150 meV with

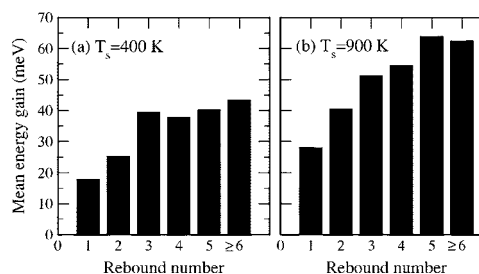


FIG. 6. Energy gain by  $H_2$  molecules reflected from a Pd(111) surface as a function of the rebound number. The impact energy is 10 meV. The surface temperature  $T_s$  is 400 K (a) and 900 K (b).

respect to the rigid surface case, confirming the absence of temperature effects in this energy region. However, a large difference now appears below 150 meV.

Various factors may contribute to the isotopic effect. One

is related with the ZPE of the molecule in the entrance channel. As already explained above, our calculations account for the variation of ZPE energy in the approach toward the surface through an additional term in the PES of the form

$$\text{ZPE} = \begin{cases} \text{ZPE}^0, & \text{if } Z \geq Z_2 \\ \text{ZPE}^0 - \Delta/2 + \Delta/2 \cos[\pi(Z - Z_2)/(Z_2 - Z_1)], & \text{if } Z_1 < Z < Z_2; \\ \text{ZPE}^0 - \Delta, & \text{if } Z \leq Z_1; \end{cases} \quad (5)$$

where  $Z_1$  is 0.7 Å (resp. 1 Å) and  $Z_2=2.7$  Å (resp. 3 Å) for Pd(110) [resp. Pd(111)]. The coefficient  $\Delta$  is equal to 60 meV for  $\text{H}_2$ , 42.4 meV for  $\text{D}_2$ , and 34.6 meV for  $\text{T}_2$ . It is the only mass effect for the case of the rigid surface [Fig. 7(a)], which leads us to conclude that the isotopic effect above 150 meV in Fig. 7(b) is entirely due to the ZPE change.

For the low-energy range, two additional effects come into play. For a given impact energy, the evolution time scales like the square root of the mass, i.e., the evolution is slower for heavier projectiles. In addition, the mass ratio between surface atoms and projectile changes. As we already know that the ZPE change does not play a role at low energies [see Fig. 7(a)], we have to find a way to discriminate between the last two factors. The easiest way to do it is to make calculations for  $\text{H}_2$  while changing the surface atom mass and conserving the same value for the SO vibration frequency. In this way the evolution time scale (both for the projectile dynamics and surface vibrations) remains unchanged. We did calculations with a surface atom mass divided by 2, which should be compared with our previous results for  $\text{D}_2$  impact, and by 10. Results are plotted in Fig. 7(b). One notes immediately that the results for a surface atom mass divided by two are nearly identical to those for  $\text{H}_2$ . This proves definitively that the main factor is the time scale and *not* the mass ratio! This conclusion is confirmed by

calculations with the surface atom mass divided by 10. In spite of this large reduction, results are very close to those for  $\text{H}_2$  and much closer to  $\text{H}_2$  than those for  $\text{T}_2$ .

As the above conclusion contradicts the usual statement on the role of the mass ratio in energy exchange with the surface, it should be made clear that our argument concerns a *hot* surface. Indeed, it is easy to understand why this is so in the latter case. The typical surface vibration time is 0.25 ps. If the process of interest takes place over a time much shorter than the latter value, the projectile does not see any surface motion. However, if the reaction time is of the order of the vibration time, then the projectile, whatever the value of its mass, evolves in an “external” time-dependent potential that causes energy exchange. The absolute value of the projectile mass (not its ratio to the surface atom one) is one factor determining the reaction time. However, much more significant is the occurrence of a mechanism, increasing the interaction time with the surface like dynamic trapping. The interpretation of Fig. 7 for low energies is now clear. Because of the increase in reaction time,  $\text{D}_2$  exchanges energy more efficiently than  $\text{H}_2$  with the surface. We have shown above that, for the case of a *hot* surface, energy flows from the surface to the adsorbate, which allows dynamically trapped molecules to go back into the vacuum, hence a decrease in dissociation. This phenomenon is even larger for  $\text{T}_2$ .

The situation is different for a “cold” surface. Then, the amplitude of surface vibrations is small, hence that of the potential temporal variation. The consequence is shown in Fig. 8: the mass effect is much smaller than for the hot surface. In addition, for a *cold* surface, energy flows from the molecule toward the SO, which increases dissociation.

### C. GLO model

One limitation of the SO model is that energy dissipation to the bulk is not considered. This might be a serious shortcoming when the energy exchanged with the SO is large compared with  $k_B T_s$ , and the interaction time is longer than the typical one for energy dissipation to the bulk. Our classical trajectory calculations show that this is most likely to arise for low impact energies and low surface temperatures. Therefore, we have also carried out calculations within the GLO model that incorporates dissipation effects. We present

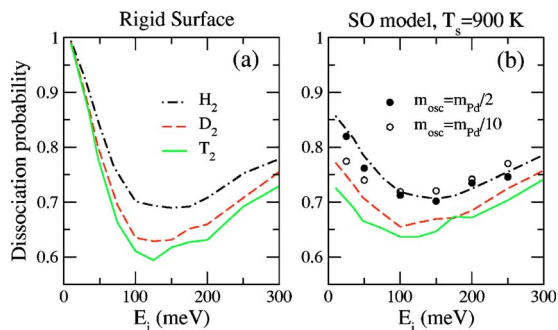


FIG. 7. (Color online) Dissociation probability for  $\text{H}_2$ ,  $\text{D}_2$ , and  $\text{T}_2$  on Pd(110) for the rigid surface (a) and surface oscillator (b) models. The SO calculation is for  $T_s=900$  K. Full (resp. open) circles are calculations for  $\text{H}_2$  with the surface atom mass divided by 2 (resp. 10).

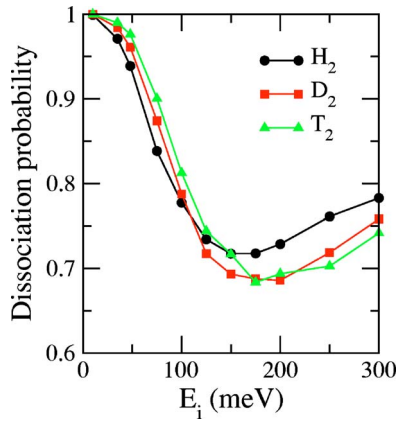


FIG. 8. (Color online) Dissociation probability for  $H_2$ ,  $D_2$ , and  $T_2$  on Pd(110) in the surface oscillator (SO) models. The surface temperature,  $T_s$ , is 10 K.

in Table I our results for adsorption on the (110) surface calculated from the fraction of trajectories that do not lead to reflection. It is clear that the total adsorption probability,  $P_{ads}$ , and the contribution of trapping to adsorption,  $P_{ads}^{trap}$ , from GLO calculations agree closely with the SO ones. Similar results are obtained for the (111) surface. Therefore, the conclusions of Sec. III B remain unchanged.

However, a closer inspection of our GLO trajectory calculations for Pd(110) shows the surprising appearance of a new adsorption channel with high probability: molecular adsorption! Indeed, we find trajectories for which the molecule remains close to the surface without dissociating after  $\sim 45$  ps, a very long time compared to the average one associated with dissociation through trapping in the SO calculations. Furthermore, at this time, all trajectories are confined within a small volume of configuration space. The corresponding *final state* is that of a molecule in a potential well over the top site or within approximately  $0.6 \text{ \AA}$  of the top site along the  $Y$  axis.<sup>46</sup> The molecular geometry associated with the PES well corresponds to  $r \sim 0.8\text{--}0.85 \text{ \AA}$ ,  $Z \sim 1.4\text{--}1.7 \text{ \AA}$ ,  $\theta \sim \pi/2$ , whereas the large range of possible  $\phi$  values shrinks as one gets away from the top site. We have verified

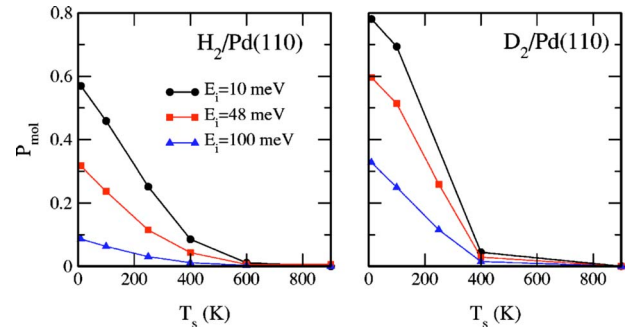


FIG. 9. (Color online) Molecular adsorption probability as a function of temperature for various impact energies  $E_i$ .  $H_2$ : left panel,  $D_2$ : right panel.

that the well is a true local minimum in six dimensions. The existence of such minima has been postulated for many years and referred to as precursor states. Dong *et al.* were the first to find them in *ab initio* calculations and to study their geometry for  $H_2/Pd(111)$ <sup>42</sup> and  $H_2/Pd(110)$ .<sup>43</sup> The present one is  $\sim 350$  meV deep with respect to the minimum value of the  $H_2$  potential in vacuum.

We give in Table I and Fig. 9 the probability,  $P_{mol}$ , of molecular adsorption. By definition, this probability corresponds to a fraction of the adsorption probability associated with trapping. The total adsorption probability associated with trapping,  $P_{ads}^{trap}$ , is the sum of  $P_{mol}$  and the dissociation probability,  $P_{diss}^{trap}$ . As we have noted above, it agrees completely with the SO result. Therefore, molecular adsorption is a direct consequence of the dissipation added in the GLO calculations. In fact, in the SO model, the conservation of energy allows an energy exchange to and from the surface. So even if a molecule may be temporarily trapped into the “precursor” well, it will eventually regain enough energy to leave the well and dissociate. The only way that a similar process may take place in the GLO is through thermal fluctuations that have a much longer characteristic time.

Molecular adsorption decreases sharply when either  $E_i$  or  $T_s$  increase. As  $E_i$  increases, not only does the energy to be dissipated in molecular adsorption increase but dynamic

TABLE I. Probability of  $H_2$  adsorption (dissociative or molecular) on a Pd(110) surface for various initial energies and surface temperatures using the surface oscillator (SO) and generalized Langevin oscillator (GLO) models. Results for a rigid surface (RS) are included for the sake of comparison.  $P_{ads}$ : total adsorption,  $P_{ads}^{trap}$ : adsorption mediated by dynamic trapping,  $P_{mol}$ : molecular adsorption.

		$T_s = 10$ K		$T_s = 100$ K		$T_s = 400$ K		$T_s = 900$ K		
		SO	GLO	SO	GLO	SO	GLO	SO	GLO	RS
$E_i = 10$ meV	$P_{ads}$	1.00	1.00	0.99	0.99	0.94	0.93	0.86	0.83	0.99
	$P_{ads}^{trap}$	0.87	0.87	0.86	0.86	0.79	0.78	0.69	0.67	0.86
	$P_{mol}$	—	0.57	—	0.46	—	0.09	—	0.00	—
$E_i = 48$ meV	$P_{ads}$	0.94	0.96	0.92	0.94	0.85	0.86	0.79	0.78	0.85
	$P_{ads}^{trap}$	0.68	0.70	0.66	0.68	0.59	0.59	0.50	0.50	0.56
	$P_{mol}$	—	0.32	—	0.24	—	0.04	—	0.00	—
$E_i = 100$ meV	$P_{ads}$	0.78	0.82	0.76	0.79	0.74	0.76	0.72	0.72	0.70
	$P_{ads}^{trap}$	0.36	0.39	0.34	0.38	0.32	0.34	0.29	0.30	0.28
	$P_{mol}$	—	0.09	—	0.06	—	0.01	—	0.00	—



trapping—the process that allows enough energy loss to produce molecular adsorption—decreases rapidly (see Fig. 9). When  $T_s$  increases, dynamic trapping decreases and simultaneously a *hotter* surface provides more energy to dynamically trapped molecules, as we have seen in Sec. III B, which enhances desorption and dissociation. For the (111) surface, molecular adsorption is much less important. For instance, for  $E_i=10$  meV and  $T_s=10$  K,  $P_{mol}=0.03$ , i.e., much smaller than the value of 0.56 obtained for the (110) surface. The higher reactivity of the (111) surface PES entails that the vast majority of trapped molecules dissociate before dissipating enough energy to get molecularly adsorbed.

The question then arises of the possibility to observe adsorbed molecules on the (110) surface. A discussion has already been given in Ref. 41 and it will not be repeated here. The crucial parameter is the lowest barrier that the molecule has to overcome to leave the precursor state. We found a height of 200 meV above the well bottom on a path leading to dissociation, which should be compared with the desorption energy of  $\sim 350$  meV. So, heating of the surface should produce dissociation of the chemisorbed molecules rather than desorption.

#### IV. CONCLUSIONS

We have shown how the surface oscillator model allows us to understand how surface temperature effects come into play when studying nonactivated dissociation of a light molecule like  $H_2$ . The most striking conclusion is that temperature effects are closely related to dynamic trapping. Although a slight effect might also be observed in direct processes, it should be kept in mind that there is not a clear-cut separation between direct and trapped trajectories and that direct trajectories include those that have rebounded up to five times on the surface. When the molecule is “hot” with respect to the surface, in the course of the dynamic trapping process, energy is lost to the surface. This enhances the trapping effect and, therefore, the dissociation probability. On the other

hand, if the molecule is “cold” with respect to the surface, it gains energy from phonons, which quenches trapping and increases reflection. All the features that we have observed in our calculations can be understood in terms of this simple picture. We have shown that some experimental observations give weight to our interpretation.

It has been generally considered that the mass mismatch between the molecule and surface atoms can be used as a criterion to justify the rigid surface model. Actually, we find that this is not a valid argument as far as hot surfaces are concerned. In the latter case, the key factor is the reaction time compared to a typical surface vibration time. In a fast reaction, the molecule does not see any surface motion and temperature effects are weak. The maximum energy exchange will take place when both times are comparable.

Finally, we have shown that the surface oscillator model reaches a limit when dissipation of energy to the bulk is a relevant issue. We have used a generalized Langevin oscillator to account for dissipation from the surface oscillator to the bulk. While this has no consequence in global sticking and reflection rates, it opens the possibility of molecular adsorption into a “precursor” well. These molecular adsorption states decay toward dissociation and should only be observed at low surface temperature because: (i) a cold surface is required so that the molecule will lose energy; (ii) the precursor states may be depopulated if the barrier of 200 eV can be overcome.

Although we do not pretend that the surface oscillator model might be considered as an accurate representation of phonon effects, the results of the present work allow us to gain some useful insight into the circumstances under which the latter are likely to play an important role. A preliminary study with a rigid surface may be sufficient in many cases to establish if surface temperature might play a role or not.

#### ACKNOWLEDGMENTS

This work has been partially supported by the bilateral France-Argentina ECOS-Sud Project No. A03E04.

\*Corresponding author. Electronic address: busnengo@ifir.edu.ar

<sup>1</sup>A. Gross, Surf. Sci. Rep. **32**, 291 (1998).

<sup>2</sup>G. Kroes, Prog. Surf. Sci. **60**, 1 (1999).

<sup>3</sup>K. Christmann, Surf. Sci. Rep. **9**, 1 (1988).

<sup>4</sup>G. R. Darling and S. Holloway, Rep. Prog. Phys. **58**, 1595 (1995).

<sup>5</sup>E. Watts and G. O. Sitz, J. Chem. Phys. **111**, 9791 (1999).

<sup>6</sup>E. Watts and G. O. Sitz, J. Chem. Phys. **114**, 4171 (2001).

<sup>7</sup>H. A. Michelsen, C. T. Rettner, and D. J. Auerbach, Surf. Sci. **272**, 65 (1992).

<sup>8</sup>M. J. Murphy and A. Hodgson, J. Chem. Phys. **108**, 4199 (1998).

<sup>9</sup>J. C. Polanyi and R. J. Wolf, J. Chem. Phys. **82**, 1555 (1985).

<sup>10</sup>M. Hand and J. Harris, J. Chem. Phys. **92**, 7610 (1990).

<sup>11</sup>M. Dohle and P. Saalfrank, Surf. Sci. **373**, 95 (1997).

<sup>12</sup>M. Dohle, P. Saalfrank, and T. Uzer, Surf. Sci. **409**, 37 (1998).

<sup>13</sup>B. Jackson, Chem. Phys. Lett. **308**, 456 (1999).

<sup>14</sup>H. P. Steinrück, M. Luger, A. Winkler, and K. D. Rendulic, Phys. Rev. B **32**, 5032 (1985).

<sup>15</sup>H. F. Berger, C. Resch, E. Grösslinger, G. Eilmsteiner, A. Winkler, and K. D. Rendulic, Surf. Sci. Lett. **275**, L627 (1992).

<sup>16</sup>D. A. Butler and B. E. Hayden, Chem. Phys. Lett. **232**, 542 (1995).

<sup>17</sup>K. D. Rendulic, A. Winkler, and H. Karner, J. Vac. Sci. Technol. A **5**, 488 (1987).

<sup>18</sup>J. E. Müller, Phys. Rev. Lett. **59**, 2943 (1987).

<sup>19</sup>D. Butler, B. E. Hayden, and J. D. Jones, Chem. Phys. Lett. **217**, 423 (1994).

<sup>20</sup>C. Resch, H. F. Berger, K. D. Rendulic, and E. Bertel, Surf. Sci. **316**, L1105 (1994).

<sup>21</sup>D. Butler and B. E. Hayden, Surf. Sci. **337**, 67 (1995).

<sup>22</sup>M. Beutl, M. Riedler, and K. D. Rendulic, Chem. Phys. Lett. **247**, 249 (1995).



- <sup>23</sup>A. Gross, S. Wilke, and M. Scheffler, Phys. Rev. Lett. **75**, 2718 (1995).
- <sup>24</sup>M. Kay, G. R. Darling, S. Holloway, J. A. White, and D. M. Bird, Chem. Phys. Lett. **245**, 311 (1995).
- <sup>25</sup>A. Gross and M. Scheffler, Phys. Rev. B **57**, 2493 (1998).
- <sup>26</sup>G. R. Darling, M. Kay, and S. Holloway, Surf. Sci. **400**, 314 (1998).
- <sup>27</sup>M. Beutl, J. Lesnik, K. D. Rendulic, R. Hirschl, A. Eichler, G. Kresse, and J. Hafner, Chem. Phys. Lett. **342**, 473 (2001).
- <sup>28</sup>C. Crespos, H. F. Busnengo, W. Dong, and A. Salin, J. Chem. Phys. **114**, 10954 (2001).
- <sup>29</sup>H. F. Busnengo, C. Crespos, W. Dong, J. C. Rayez, and A. Salin, J. Chem. Phys. **116**, 9005 (2002).
- <sup>30</sup>H. F. Busnengo, E. Pijper, M. F. Somers, G. J. Kroes, A. Salin, R. A. Olsen, D. Lemoine, and W. Dong, Chem. Phys. Lett. **356**, 515 (2002).
- <sup>31</sup>M. A. DiCésare, H. F. Busnengo, W. Dong, and A. Salin, J. Chem. Phys. **118**, 11226 (2003).
- <sup>32</sup>H. F. Busnengo, E. Pijper, G. J. Kroes, and A. Salin, J. Chem. Phys. **119**, 12553 (2003).
- <sup>33</sup>H. F. Busnengo, W. Dong, P. Sautet, and A. Salin, Phys. Rev. Lett. **87**, 127601 (2001).
- <sup>34</sup>C. Díaz, F. Martín, H. F. Busnengo, and A. Salin, J. Chem. Phys. **120**, 321 (2004).
- <sup>35</sup>H. F. Busnengo, A. Salin, and W. Dong, J. Chem. Phys. **112**, 7641 (2000).
- <sup>36</sup>J. C. Tully, J. Chem. Phys. **73**, 1975 (1980).
- <sup>37</sup>J. Stoer and R. Burlisch, *Introduction to Numerical Analysis* (Springer-Verlag, New York, 1980).
- <sup>38</sup>D. Beeman, J. Comput. Phys. **20**, 130 (1976).
- <sup>39</sup>J. C. Tully, G. H. Gilmer, and M. Shugard, J. Chem. Phys. **71**, 1630 (1979).
- <sup>40</sup>S. A. Adelman and J. D. Doll, J. Chem. Phys. **64**, 2375 (1976).
- <sup>41</sup>H. F. Busnengo, W. Dong, and A. Salin, Phys. Rev. Lett. **93**, 236103 (2004).
- <sup>42</sup>W. Dong and J. Hafner, Phys. Rev. B **56**, 15396 (1997).
- <sup>43</sup>V. Ledentu, W. Dong, and P. Sautet, Surf. Sci. **412/413**, 518 (1998).
- <sup>44</sup>Experimentally, the study of  $T_s$  effects in the initial adsorption probability (low coverage limit) for highly reactive systems faces with difficulties since, for small  $T_s$ , a layer of H atoms builds up. Its determination is therefore restricted to  $T_s$  values above the desorption temperature (e.g.,  $\sim 400$  K for Pd).
- <sup>45</sup>An additional change is due to the fact that we make use of an initial ensemble of oscillator velocities reproducing a Maxwellian distribution. However, the corresponding change in relative impact energy is negligible due to the small mass ratio between  $H_2$  and Pd.
- <sup>46</sup>The PES is rather shallow in the latter region. A comparison between *ab initio* and interpolated data show that, in spite of the accuracy of the CRP ( $\sim 15$  meV), the absolute minimum is displaced in the CRP data with respect to the true *ab initio* minimum located over the top. This small difference is immaterial as far as dynamical aspects are concerned.